Noname manuscript No.
(will be inserted by the editor)

Estimating cooling production and monitoring efficiency in chillers using a soft sensor

Serafín Alonso · Antonio Morán · Daniel Pérez · Miguel A. Prada · Ignacio Díaz · Manuel Domínguez

Received: date / Accepted: date

Abstract Intensive use of heating, ventilation and air conditioning (HVAC) systems in buildings entails monitoring their efficiency. Moreover, cooling systems are key facilities in large buildings and can account up to 44% of the energy consumption. Therefore, monitoring efficiency in chillers is crucial and, for that reason, a sensor to measure the cooling production is required. However, manufacturers rarely install it in the chiller due to its cost. In this paper, we propose a methodology to build a *soft sensor* that provides an estimation of cooling production and enables monitoring the chiller efficiency. The proposed soft sensor uses independent variables (internal states of the chiller and electric power) and can take advantage of current or past observations of those independent variables. Six methods (from linear approaches to deep learning ones) are proposed to develop the model for the soft sensor, capturing relevant features on the structure of data (involving time, thermodynamic and electric variables and the number of refrigeration circuits). Our approach has been tested on two different chillers (large water-cooled and smaller air-cooled chillers) installed at the Hospital of León. The methods to implement the soft sensor are assessed according to 3 metrics (MAE, MAPE and R^2). In addition to the comparison of methods, the results also include the estimation

This work was supported in part by the Spanish Ministerio de Ciencia e Innovación (MICINN) and the European FEDER funds under project CICYT DPI2015-69891-C2-1-R/2-R.

S. Alonso, A. Morán, D. Pérez, M. A. Prada, M. Domínguez
Grupo de investigación en Supervisión, Control y Automatización de Procesos Industriales (SUPPRESS), Esc. de Ing. Industrial, Informática y Aeroespacial, Universidad de León, Campus de Vegazana s/n, 24007, León, Spain.
Tel.: +987291694
E-mail: {saloc, a.moran, dperl, ma.prada, manuel.dominguez}@unileon.es

I. Díaz
Electrical Engineering Department, University of Oviedo, Edif. Departmental 2, Campus de Viesques s/n, Gijón 33204 Spain
E-mail: idiaz@uniovi.es

of cooling production (and the comparison of the true and estimated values) and monitoring the COP indicator for a period of several days and for both chillers.

Keywords HVAC systems · Chillers · Efficiency · Cooling production · Soft sensor · Deep learning

1 Introduction

The proliferation of heating, ventilation and air conditioning (HVAC) systems has caused a noticeable increase of energy consumption in buildings. Nowadays, it represents more than 20% of global energy consumption in developed countries [40]. Most of that energy consumption is due to the air conditioning systems, which consume up to 44% of the total energy consumption in commercial and industrial buildings [43, 47]. The main element of those systems is the chiller, which is in charge of removing heat from inside the buildings by means of electric power. Therefore, its performance is vital in order to achieve energy efficiency of these buildings.

Chiller efficiency requires the computation of an *energy efficiency indicator* (EEI) [4]. Most of them use the measurement of the cooling production (i.e., the chiller output). For that purpose, a meter inserted in the output pipe could be used to obtain the cooling production with very low errors [33]. However, an energy meter is invasive and involves installation, maintenance and recalibration costs [34], so manufacturers do not usually include it in their chillers.

The energy meter can be replaced by a soft sensor [30], achieving a trade-off between the accuracy of measurements and the cost of the sensor. For that reason, in this paper, we propose the development of a soft sensor to estimate the cooling production in chillers and to monitor its efficiency. The main contributions of this paper are:

- A methodology for estimating cooling production and efficiency in chillers, based on independent variables, without installing a cooling power meter.
- The development of a soft sensor that provides cooling production measurements, based on current and past observations of internal refrigeration variables and electric consumption.
- The validation and comparison of different alternative models, used to build the soft sensor.
- Testing the approach and the soft sensor measurements using data from different real chillers.
- Monitoring the actual efficiency of different real chillers.

This paper is organized as follows: Section 3 explains the motivations for measuring the cooling production in chillers. In Section 4, the proposed methodology to build the soft sensor is presented. Section 5 describes the chillers used for experimentation, the datasets and the proposed experiments. In Section 6, the results are exposed and discussed. Finally, conclusions are drawn in Section 7.

2 Literature review

Virtual or *soft* sensing is a low cost and non-invasive method to obtain measurements indirectly that can provide further information from the system. Generally, a soft sensor can be obtained using a model suitable to estimate interesting parts without putting real sensors [31]. On one hand, these models can be developed taking into account ideal states of the processes [28], e.g. Kalman filters estimate state variables that define system dynamics. On the other hand, data-based models can improve the description of process conditions because they consider more realistic situations that can occurred in the process.

Soft sensors have been applied to estimate variables in many industrial applications [28]. However, there are other domains such as building systems where this approach is slowly adopted. In this sense, virtual sensing developments can provide improvements in terms of monitoring, diagnostics and optimization in buildings [30]. Heating, Ventilating and Air Conditioning (HVAC) systems are widely used for thermal comfort in buildings and chillers are essential parts of these systems, playing a significant role in terms of consumption, maintenance and operational costs. For this reason, a number of previous works have addressed the study of virtual models that obtain features from chillers, such as the estimation of water flow rates [58, 50, 35], identification of various faults [36, 41, 53] or cooling load measurements [25, 26]. In this work, a methodology for a data-based soft sensor is proposed to estimate cooling production in chillers using explanatory variables.

Various strategies for developing soft sensors have been proposed, such as neural networks [7] or principal component analysis [27], and they have also been applied to model systems composed by chillers [52, 6]. For instance, the estimation of steady-state performance in chillers based on radial basis functions was proposed to identify dynamic conditions [46, 5]. Moreover, optimal sequence for chiller operation was determined by estimating power consumption [10] and empirical models using historical data were proposed although their parameters cannot be easily extrapolated [51, 13]. However, our proposed approach relies on a data-based model that can be extrapolated to similar devices and focuses on monitoring the efficiency of one chiller instead of sequencing a group of chillers in a plant. In [48], a neural network is proposed to predict the efficiency of screw chillers using the COP with $\pm 5\%$ error, whereas our work relies on internal variables and compares further configurations including deep learning approaches in order to obtain enhanced results.

Recent deep learning approaches have provided significant advances in neural networks that can learn representations with higher levels of abstraction from data [20]. Several methods have been proposed for feature engineering in order to improve building energy prediction [15]. Moreover, deep learning approaches have also been explored for cooling load prediction in buildings, compared with other traditional methods in [16] and used in a hybrid model with ensemble method in [17] in order to deal with uncertainties.

However, deep learning approaches have been rarely applied to estimate an output from a soft sensor and they could provide further features that allow to obtain more complex models. Accordingly, a virtual sensor for cooling power estimation is suggested in [3] using a deep convolutional neural network that has obtained promising results compared to other methods, using internal variables of three refrigeration circuits from one real chiller in a hospital facility. An extension of that work is presented here, including temporal information of explanatory variables and considering two chillers with different structure and operational baselines. Furthermore, additional deep learning methods are used in order to build a soft sensor that estimates cooling production and allows monitoring the efficiency in chillers. These estimations can avoid the use of industrial meters whose installation and maintenance would increase costs.

Previous works mentioned above have explored soft sensors in buildings to improve the efficiency, considering different chiller configurations, sequencing operations or a variety of variables. However, the soft sensor proposed here estimates cooling production based on internal variables (gas pressures and temperatures) and electric power from each refrigeration circuit in the chiller. It can be used for other chillers in a similar way. Several methods are compared, including deep learning networks that have proven to be an advanced tool to predict energy in buildings [16] and they can be a helpful option to build valuable soft sensors.

3 How to monitor chiller efficiency

A chiller is an HVAC system in charge of providing cooling power to building facilities. It converts electric power (input) into cooling power (output). For that purpose, the chiller comprises one or more refrigeration circuits (see Fig. 1) which are used to absorb heat from water or glycol and transfer it to the atmosphere, based on a refrigeration thermodynamic cycle. Electric power is required to modify the conditions of the refrigeration gas (evaporating and condensing temperatures and pressures) [21]. The efficiency of a chiller is defined as the ratio between the cooling production (output) and the electric power (input) [4], i.e,

$$\text{Efficiency} = \frac{\text{Cooling Power (output)}}{\text{Electric Power (input)}}. \tag{1}$$

Electric power can be easily measured, since most of the chillers include current sensors in order to control their capacity in terms of full load amperes (FLA) and the rated compressor power [56]. On the contrary, cooling power requires a specific flow meter and two temperature sensors, whose installation is a drawback due to the invasive measuring principle and the increase of cost. Moreover, its measurements could be affected negatively by outside conditions. As a result, manufacturers rarely include cooling power meters in their chillers, hindering efficiency monitoring.

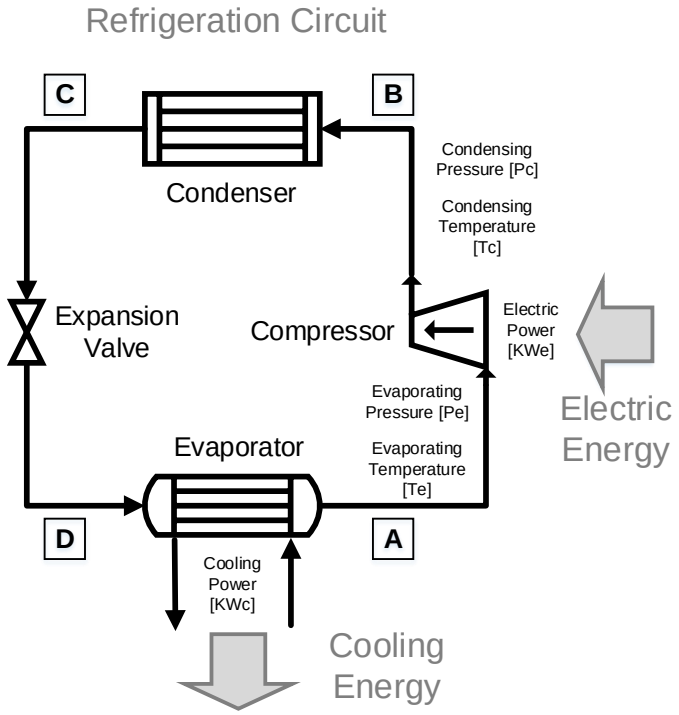

Fig. 1: A typical refrigeration circuit.

Normally, a chiller is formed by several refrigeration circuits, with similar or different capacities, in order to achieve a better adaptation to variable cooling loads [45]. Each individual circuit provides cooling power according to a central chiller control. Thus, the total cooling production of the chiller is the sum of the cooling power from each circuit c, i.e.

$$\text{Cooling Power } (KWc) = KWc_1 + KWc_2 + \ldots + KWc_c. \tag{2}$$

In the same way, total electric power demanded by the chiller is the sum of the electric power from each circuit c, i.e.

$$\text{Electric Power } (KWe) = KWe_1 + KWe_2 + \ldots + KWe_c. \tag{3}$$

Typically, chiller manufacturers use the COP (*coefficient of performance*) indicator as the efficiency ratio, providing theoretical values for given surrounding conditions during the manufacturing process [57]. However, chiller efficiency varies over time and depends on external conditions [55], so it is essential to monitor this performance indicator. COP values can be easily computed using the total cooling power and electric power [4] (see Eq. 4).

$$COP = \frac{KWc}{KWe} = \frac{\sum_{i=1}^{n} KWc_i}{\sum_{i=1}^{n} KWe_i} \quad \forall i \in [1, c] \tag{4}$$

In a refrigeration circuit, the COP indicator depends mainly on enthalpies H (given the type of refrigeration gas) [32]. To justify this claim, let us perform an analysis of a theoretical refrigeration cycle, where the energy conservation equation ($Q - W = \Delta H$) is applied for each element [29]. Any system interchanges heat Q or work W with the environment, being the balance equal to the variation of enthalpies ΔH. For the evaporator, we have $W = 0$, so $Q = \Delta H$. Looking at Fig. 1, points D and A represent the input and the output of the evaporator, so $Q = H_D - H_A$. On the other hand, the compressor performs an adiabatic process ($Q = 0$), so $-W = \Delta H$. Considering the input point (A) and the output point (B) in this case (see Fig. 1), the compressor work is $W = H_A - H_B$. Analyzing the condenser, we have $W = 0$, so $Q = \Delta H$. Obtaining the enthalpies of the input (point B) and the output (point C) (see Fig. 1), it can be seen that $Q = H_C - H_B$ in the condenser. Finally, applying the energy balance in the expansion valve, we have $Q = 0$ and $W = 0$, so $\Delta H = 0$. It means that enthalpies before and after this element must be equal, i.e. $H_D = H_C$ (see Fig. 1).

According to the previous energy analysis, the COP value can be defined as follows [38]:

$$COP = \frac{Q_{Evaporator}}{W_{Compressor}} = \frac{H_D - H_A}{H_A - H_B} \tag{5}$$

Thus, it demonstrates that chiller performance (COP) depends on enthalpies, in the high pressure line (point B) and the low pressure line (points D and A) (see Fig. 1).

In thermodynamics, the enthalpy is defined as $H = U + PV$, being U the internal energy, P the pressure and V the volume (constant in this case) [2]. The internal energy U of a gas depends mainly on kinetic and vibration energies of molecules, i.e., on temperature and pressure. In turn, the enthalpy is a magnitude which characterizes the state of a system in equilibrium, but it does not consider how the system reaches that state [2]. Thus, enthalpies can be computed using pressures and temperatures, given a refrigeration gas. Our hypothesis is that these variables can define the state of the system.

For those reasons, the proposed soft sensor should be able to estimate the cooling production and the COP value based on independent variables in the refrigeration circuit (temperatures, pressures and electric power). A limitation of the proposed methodology is the occasional need for a portable meter to measure and record actual cooling power data (chillers do not usually include such a meter) under a range of conditions for training and testing purpose, together with the computational resources needed for that. Furthermore, that process might require scheduled retraining after long periods to suit potential changes in the chiller dynamics due to maintenance or wear.

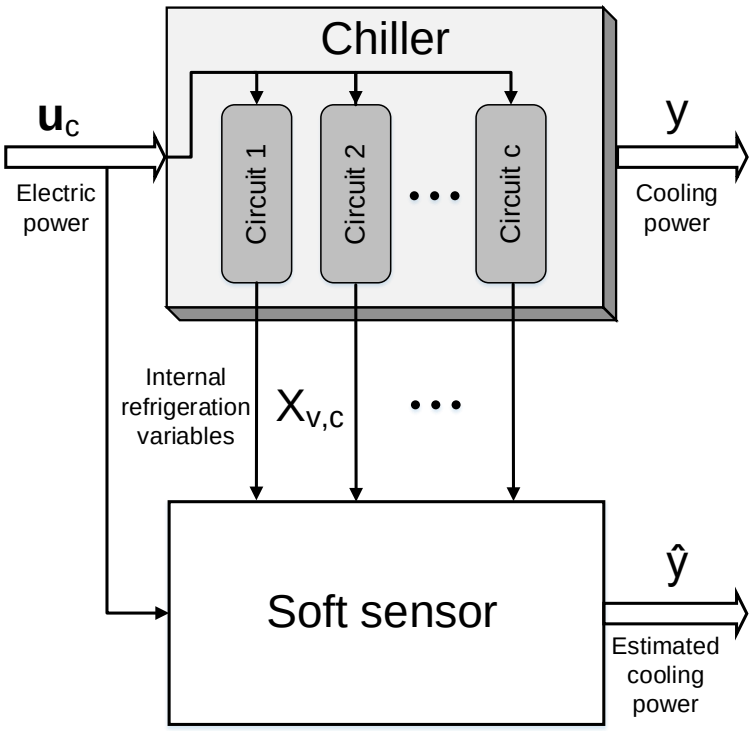

Fig. 2: Proposed approach based on a soft sensor to estimate cooling production.

4 Methodology

4.1 Requirements and structure of the soft sensor

We propose a methodology for estimating the cooling production in chillers from the available variables in the chiller control system, such as energy inputs and internal states of the refrigeration circuits (see Fig. 2). To estimate the cooling production, we develop a soft sensor which uses those variables to provide accurate values of the cooling production and allow us to estimate chiller efficiency. The challenge is to obtain a model for the soft sensor that is able to yield outputs with a low error.

Based on the considerations exposed in section 3, the proposed approach should take into account the following aspects in order to address the regression problem:

– A chiller unit can comprise several refrigeration circuits, which provide cooling power.

- Cooling power and efficiency depend on the energy input (compressor work) and the state of the refrigeration circuits, which is defined by internal variables (pressures and temperatures of gas).
- Past inputs and states of the refrigeration circuits (not only the current ones) can also influence the cooling power and efficiency, due to the thermodynamic inertias as well as the time that a gas molecule spends in going around the circuit (higher in large chillers with longer pipes).
- Dependencies among variables are expected in the same circuit since the refrigeration cycle is closed.
- Interactions among refrigeration circuits could appear depending on the chiller manufacturing structure.

Therefore, the cooling production of a refrigeration circuit can be defined as a function f of the current and past energy inputs and the internal variables (see Eq. 6).

$$\hat{y}(t) = f\left(\boldsymbol{\Phi}_{v,c,t}\right) \tag{6}$$

$\hat{y}(t)$ is the estimated cooling production of the chiller and $\boldsymbol{\Phi}_{v,c,t}$ is a tensor with three dimensions: variables (v), circuits (c) and time (t).

To understand $\boldsymbol{\Phi}_{v,c,t}$ let us first define $\mathbf{u}_c$ as a vector with the power inputs to each circuit $c \in [1, \ldots, q]$ (mainly the compressor work), i.e.,

$$\mathbf{u}_c = [u_1, u_2, \ldots, u_q]\,. \tag{7}$$

Let also $X_{v,c}$ be a matrix containing the internal variables $v \in [1, \ldots, p]$ (temperatures and pressures of the refrigeration gas) for each circuit $c \in [1, \ldots, q]$. Its dimensions will then be variables $\times$ circuits (p, q), i.e.,

$$X_{v,c} = \begin{bmatrix} x_{11} & x_{12} & \ldots\ldots & x_{1q} \\ x_{21} & x_{22} & \ldots\ldots & x_{2q} \\ \ldots & \ldots & \ldots\ldots & \ldots \\ x_{p1} & x_{p2} & \ldots\ldots & x_{pq} \end{bmatrix}. \tag{8}$$

It is possible to define a matrix $\Phi_{v,c}$ that includes both $\mathbf{u}_c$ and $X_{v,c}$ and therefore has dimensions $(p+1, q)$. But, since our approach should also consider the system dynamics (t), i.e., how past inputs and states of the circuits influence the cooling production, current ($t_0 = k$) and past observations ($t_1 = k-1, t_2 = k-2, \ldots, t_n = k-n$) of inputs and states are introduced in the model. Therefore, we can rewrite the Eq. 6 as follows:

$$\hat{y}(k) = f\Big(\Phi_{v,c}(k), \Phi_{v,c}(k-1), \ldots, \Phi_{v,c}(k-n)\Big) \tag{9}$$

where, for a given instant of time k, matrix Φ is

$$\Phi_{v,c}(k) = [\mathbf{u}_c, X_{v,c}]_{(k)} = \begin{bmatrix} u_1 & u_2 & \ldots\ldots & u_q \\ x_{11} & x_{12} & \ldots\ldots & x_{1q} \\ x_{21} & x_{22} & \ldots\ldots & x_{2q} \\ \ldots & \ldots & \ldots\ldots & \ldots \\ x_{p1} & x_{p2} & \ldots\ldots & x_{pq} \end{bmatrix}_{(k)}. \tag{10}$$

The above matrix $\Phi_{v,c}(k)$ can be flattened, resulting in the following vector whose length is Variables × Circuits × Time:

$$\begin{aligned}\boldsymbol{\varphi}_{vct} = \big[&\boldsymbol{\varphi}_{v1}(k), \boldsymbol{\varphi}_{v2}(k), ..., \boldsymbol{\varphi}_{vq}(k), \boldsymbol{\varphi}_{v1}(k-1), \boldsymbol{\varphi}_{v2}(k-1), ..., \\ &\boldsymbol{\varphi}_{vq}(k-1), ..., \boldsymbol{\varphi}_{v1}(k-n), \boldsymbol{\varphi}_{v2}(k-n), ..., \boldsymbol{\varphi}_{vq}(k-n)\big]^T,\end{aligned} \tag{11}$$

where $\boldsymbol{\varphi}_{v1}(k) = \big[u_1, x_{11}, x_{21}, ..., x_{p1}\big]^T$, $\boldsymbol{\varphi}_{v2}(k) = \big[u_2, x_{12}, x_{22}, ..., x_{p2}\big]^T$ and so on, for the time instant k. Analogous vectors $\boldsymbol{\varphi}_{v1}(k-n), \boldsymbol{\varphi}_{v2}(k-n), ..., \boldsymbol{\varphi}_{vq}(k-n)$ are defined for past observations at time $k-n$.

On the other hand, $\Phi_{v,c}(k)$ can be reshaped, resulting in the following matrix whose dimension is:

$$\Psi_{vc,t} = \big[\boldsymbol{\xi}_{vc}(k), \boldsymbol{\xi}_{vc}(k-1), ..., \boldsymbol{\xi}_{vc}(k-n)\big], \tag{12}$$

where

$$\begin{aligned}\boldsymbol{\xi}_{vc}(k) = \big[&u_1, x_{11}, x_{21}, ..., x_{p1}, u_2, x_{12}, x_{22}, ..., \\ &x_{p2}, ..., u_q, x_{1q}, x_{2q}, ..., x_{pq}\big]^T\end{aligned} \tag{13}$$

and $\boldsymbol{\xi}_{vc}(k-1), \boldsymbol{\xi}_{vc}(k-2), ..., \boldsymbol{\xi}_{vc}(k-n)$ have an identical structure, but contain the corresponding past observations.

4.2 Model for the soft sensor

The challenge is to achieve the model function f indicated in Eq. 9, which relates output $\hat{y}$ to a regressor formed by the input $\mathbf{u}_c$ and the internal state $X_{v,c}$. Furthermore, the model f should be as accurate as possible, in order to obtain low measurement errors, in similar ranges to those of commercial industrial energy meters.

To model f, we assess linear and nonlinear methods in order to select the best model in terms of accuracy and to delimit its error range. Prior to training the different methods, real data have to be collected and preprocessed. Then, input data needs to be prepared and transformed according to the requirements of each method. Once this comparison is performed, the most appropriate method can be implemented and deployed in the chiller plant software.

The candidate methods proposed to build the soft sensor are (see Fig. 3):

- **Multiple Linear Regression (MLR):** MLR is a method that models the relationship between two or more explanatory variables and a response variable by fitting a linear equation to observed data [22,18]. For that purpose, the values of the independent variables or regressor $(\mathbf{u}_c, X_{v,c})$ are associated with a value of the dependent variable $\hat{y}$. In this case, the input vector is $\boldsymbol{\varphi}_{vct}$ (see Eq. 11) whose length is Variables × Circuits × Time and the output value is the soft sensor measurement, i.e. the cooling production.

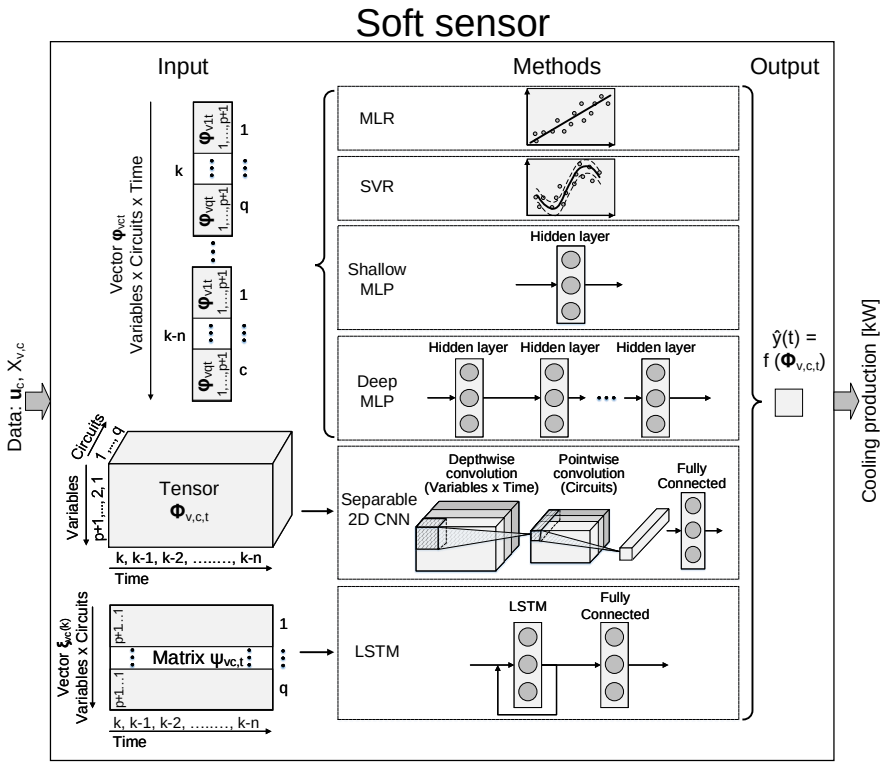

Fig. 3: Methods used to build the soft sensor.

– **Support Vector Regression (SVR):** SVR derives from Support Vector Machines and its basic idea is to map nonlinearly the data into a high-dimensional space so that a linear regression is performed in that space [14, 42]. SVR estimates the regression function f, which relates the input vector $\boldsymbol{\varphi}_{vct}$ (see Eq. 11), whose length is Variables × Circuits × Time and the output $\hat{y}$. For that purpose, a cost function is minimized, subject to certain constraints.
– **Shallow Multilayer Perceptron (Shallow MLP):** Shallow or classic MLP is a type of feedforward artificial neural network with several layers of neurons: an input layer, one or more hidden layers and an output layer [23, 39]. A nonlinear activation function is used for each neuron and the network is trained using backpropagation algorithm. In this case, only one hidden layer is defined. Input data $\boldsymbol{\varphi}_{vct}$ (see Eq. 11) is again structured as a vector of length Variables × Circuits × Time and the output $\hat{y}$ is the cooling production provided by the soft sensor.
– **Deep Multilayer Perceptron (Deep MLP):** A deep MLP, with many layers of neurons (an input layer, several hidden layers and an output layer), is also considered [12]. A nonlinear activation function is used for each

neuron. Compared to shallow MLP, the deep MLP uses a new initialization strategy in the training process to avoid the vanishing and/or exploding gradients caused by backpropagation in neural networks with many layers [20]. Similar to MLP, the input data consists of a vector $\boldsymbol{\varphi}_{vct}$ (see Eq. 11) whose length is Variables × Circuits × Time and the output $\hat{y}$ is the soft sensor measurement.

- **Separable 2D Convolutional Neural Network (2D CNN):** A separable 2D CNN is a convolutional neural network that works in two dimensions but performs its convolutions in two consecutive stages instead of one: the depthwise and pointwise convolutions [11]. In this way, the kernels are divided into two smaller ones, so that computational complexity decreases, favoring generalization and facilitating the convergence, so the network runs faster. The first (depthwise) convolution is performed over the spatial dimensions (width and height of the data) whereas the second (pointwise) convolution is performed over the number of channels of data [49]. In this particular setup, separable 2D CNN could take advantage of coherence among refrigeration circuits, variables (electric power input and internal states) and time in a chiller. For that purpose, the input data is structured as a tensor $\boldsymbol{\Phi}_{v,c,t}$ with dimensions (Variables, Circuits, Time). In the depthwise convolution, the kernels iterate only over one channel, i.e., on time (t) and variables ($\mathbf{u}_c, X_{v,c}$) of one refrigeration circuit (c), and then stack the resulting data together. The choice of kernel size is crucial since it should consider all possible pairwise combinations among both timesteps and variables. In the pointwise convolution, the kernels iterate through every single previous data point, being the depth the number of channels, i.e., the second convolution works on the refrigeration circuits (c). After the separable 2D CNN layer, a fully connected layer and an output layer with dimension 1 (soft sensor measurements) are used. A nonlinear activation function is used for all neurons.
- **Long-Short Term Memory (LSTM):** LSTM is a recurrent neural network able to process sequences of data. A LSTM layer is formed by several neurons and each unit comprises a cell, an input gate, an output gate and a forget gate. The cell is a memory of values and the gates enable the control of its memorizing process. A LSTM unit has the ability of forgetting unnecessary information, to enable storage of new input information in the cell state to decide how the output is built [24]. For that reason, LSTM could take advantage of temporal information contained into sequences of data input [1]. That is why several sequences containing the features ($\mathbf{u}_c, X_{v,c}$) for each circuit c are fed to the network. In this scenario, the length of an input vector $\boldsymbol{\xi}_{vc}$ (see Eq. 13) at a certain time step would be Variables × Circuits. However, since previous states and energy inputs should define the current behavior of the chiller, additional timesteps of the previous samples of features and circuits are provided to the input of the network with the aim of reinforcing the short-term memory process. Thus, in this case, the input data to this method is reshaped to obtain a matrix $\Psi_{vc,t}$ (see Eq. 12) whose dimensions are (Variables × Circuits, Time). In this

case, a LSTM layer with several neurons is used. After that, a fully connected layer and an output layer are used to provide cooling production $\hat{y}$ (i.e., the soft sensor measurement). Again, a nonlinear activation function is used for all neurons.

5 Experimental procedure

For the proposed experiments, datasets are collected from real operation of chillers. Data from internal variables X and energy input $\mathbf{u}$ and from cooling power y are required. These data are merged and preprocessed. Next, the proposed methods are trained and assessed to choose the best model function f for the soft sensor and to delimit its error range. Finally, the model is deployed as a soft sensor, enabling monitoring and providing the estimation of cooling production and COP computation. Note that COP is computed from the *estimated* cooling power $\hat{y}$ and the *measured* electric power KW_e.

5.1 Chillers at the Hospital of León

The chiller plant at the Hospital of León consists of two groups of chillers: 5 air-cooled and 2 water-cooled chillers. One chiller of each type is used in the experimental setup. Their internal structure can be seen in Fig 4 and is explained below.

- **Water-cooled chiller (WCC):** The water-cooled chiller (model Trane CVGF650) has a maximum cooling capacity of 650 tons (approximately 2286 kW) and includes 1 refrigeration circuit (see Fig. 4a). It is composed of a centrifugal compressor, an electronic expansion valve (EEV) and tubular heat exchangers (for evaporator and condenser). The compressor works using R134a refrigeration gas and its capacity can be regulated between 50–100% of the maximum value, by changing the angle of the turbine blades. It is driven by a three-phase induction motor (400 V; 367 KW). The condensing water flowing through the condenser is propelled to a cooling tower, which is in charge of transferring heat to the environment when the condensing water evaporates. An axial fan, driven by a three-phase induction motor (400 V; 18.5 KW) and managed by a variable speed drive helps the heat exchange. The nominal chiller COP is 6.23 (condensing temperature: 40 °C; evaporating temperature: 0 °C).
- **Air-cooled chiller (ACC):** The air-cooled chiller (model Petra APSa 400-3) has a maximum cooling capacity of 400 tons (approximately 1407 kW) and includes 3 identical refrigeration circuits (see Fig. 4b). Each one is composed of a screw compressor, an electronic expansion valve (EEV) and a condenser in V form. A common evaporator is used for the 3 circuits. The compressor, driven by a three-phase induction motor (400 V; 109 kW), has a maximum displacement of 791 m^3/h of R134a refrigeration gas. Its capacity can be regulated between 50-100 % of maximum value

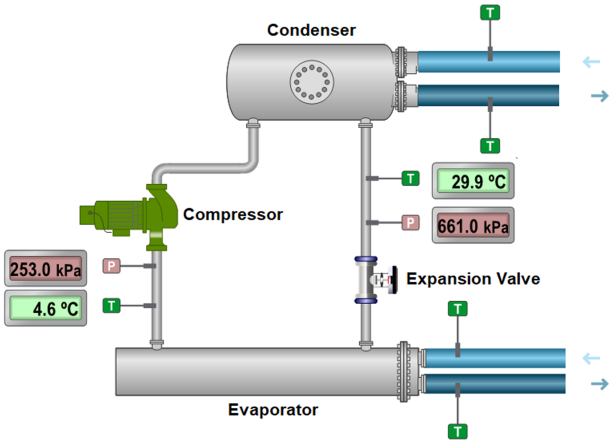

a The water-cooled chiller (WCC) with 1 refrigeration circuit.

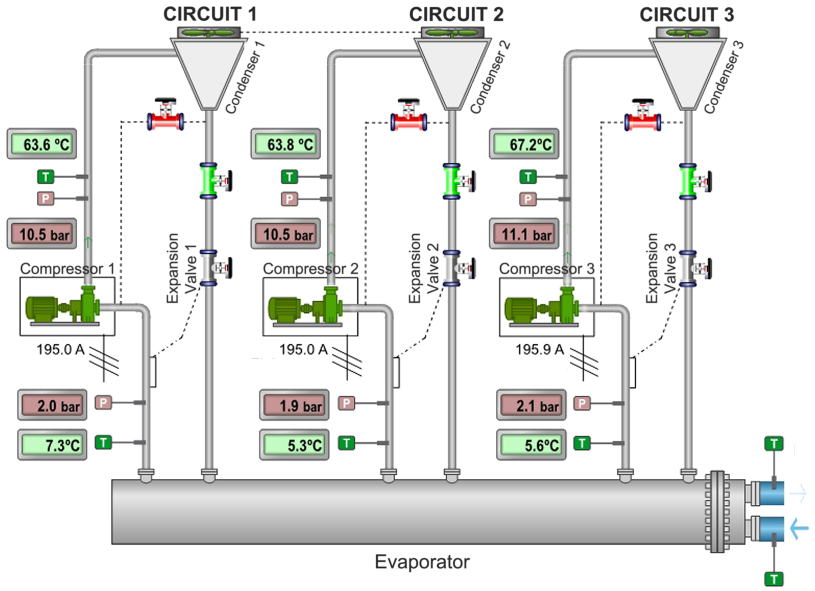

b The air-cooled chiller (ACC) with 3 refrigeration circuits.

Fig. 4: Different chillers at the Hospital of León.

by means of two auxiliary load and unload valves. The condensers have 16 fans of 1.5kW, driven by variable speed drives. Note that the condensing control signal is common to the 3 circuits. The nominal chiller COP is 4.3 (condensing temperature: 40 °C; evaporating temperature: 0 °C).

In both chillers, a control board regulates the operation of the refrigeration circuits. It communicates with a BMS (*Building Management System*), which

Table 1: Variables for each refrigeration circuit of the chillers.

Symbol	Name	Unit
Te	Evaporating temperature	$^{\circ}C$
Pe	Evaporating pressure	KPa
Tc	Condensing temperature	$^{\circ}C$
Pc	Condensing pressure	KPa
KWe	Compressor electric power	KW
KWc	Cooling power	KW

acquires and stores data from main internal variables (listed in Table 1) using Modbus protocol.

5.2 Data collection

Data are collected from two sources. First, we gather data from BMS logs (temperatures, pressures and compressor power), which stores only these data when changing in order to optimize storage capacity. BMS communicates with the chiller controller using Modbus protocol, which acquires data from sensors in the refrigeration circuits. Logs from an ultrasonic portable meter (Fluxus F601 by Flexim) are the second data source. It makes up for the lack of a cooling power meter in the chillers. The Fluxus F601 meter consists of an ultrasonic flow sensor and two Pt100 sensors (leaving and return chilled water temperatures) and provides measurements of the cooling power. This meter is configured to record cooling power data each minute. Note that the portable meter is only exceptionally used to obtain cooling power data for training and testing purposes. Both data sources (in CSV format) are preprocessed. To carry out that, data from BMS logs are resampled with 1 minute and then synchronized and merged with data from Fluxus F601 logs.

5.3 Experiments

Two experiments have been performed to test the soft sensor. For that purpose, data from both chillers at the Hospital of León were collected for 2 months, with the aforementioned sampling time of 1 minute. The selected data from the water-cooled chiller #2 (WCC2) corresponded to August and September, 2019; whereas the data from the air-cooled chiller #5 (ACC5) corresponded to December 2018 and January 2019. The resulting sizes of the datasets are $56,780$ samples for WCC2 and $38,134$ samples for ACC5. Note that the operation of these chillers is alternated with other chillers in the plant, which explains the different size of the datasets for two months. Both datasets are split into 2 parts:

– **Training and validation of the model:** In both cases, 70% of total data is used to train and validate all methods proposed to build the soft sensor. A 10-fold cross validation is applied to set the hyperparameters of each

method. Average errors and standard deviations of each 10-fold iteration have been computed.

– **Testing the soft sensor:** 30% of data (both datasets WCC2 and ACC5) is used to test the soft sensor approach by assessing the error of the cooling production estimation. For that purpose, we suppose that the F601 portable meter is disconnected from the chiller and the soft sensor is used to estimate cooling production. Finally, the chiller efficiency (COP) is computed using the estimated cooling power and the measured electric compressor power.

The estimated variable is then the cooling production KWc for all cases.

$$\hat{y} = KWc, \tag{14}$$

Five regressor variables are used: the variables T_e, P_e, T_c, P_c and energy input KWe (see Table 1) for each refrigeration circuit c. WCC2 has 1 refrigeration circuit, so using the WCC2 dataset we have

$$\mathbf{u}_c = [KWe_1], \tag{15}$$

$$X_{v,c} = [Te_1, Pe_1, Tc_1, Pc_1]^T, \tag{16}$$

$$\Phi_{v,c} = [\mathbf{u}_c, X_{v,c}] = [KWe_1, Te_1, Pe_1, Tc_1, Pc_1]^T. \tag{17}$$

In turn, for the ACC5 dataset (with 3 refrigeration circuits), we have

$$\mathbf{u}_c = [KWe_1, KWe_2, KWe_3], \tag{18}$$

$$X_{v,c} = \begin{bmatrix} Te_1 & Te_2 & Te_3 \\ Pe_1 & Pe_2 & Pe_3 \\ Tc_1 & Tc_2 & Tc_3 \\ Pc_1 & Pc_2 & Pc_3 \end{bmatrix}, \tag{19}$$

$$\Phi_{v,c} = [\mathbf{u}_c, X_{v,c}] = \begin{bmatrix} KWe_1 & KWe_2 & KWe_3 \\ Te_1 & Te_2 & Te_3 \\ Pe_1 & Pe_2 & Pe_3 \\ Tc_1 & Tc_2 & Tc_3 \\ Pc_1 & Pc_2 & Pc_3 \end{bmatrix}. \tag{20}$$

Nevertheless, our experiments should use not only current energy inputs and states of the refrigeration circuits, but also past ones, in order to consider the dynamics of the system, so instead of fitting a model for $\hat{y}(k) = f\big(\Phi_{v,c}(k)\big)$, we have

$$\hat{y}(k) = f\Big(\Phi_{v,c}(k), \Phi_{v,c}(k-1), \ldots, \Phi_{v,c}(k-n)\Big). \tag{21}$$

Table 2: Overview of the hyperparameter tuning.

Hyperparameter	Range	Best value (WCC2 model)	Best value (ACC5 model)
SVR			
ϵ-tube (ϵ)	0.001, 0.01, 0.1	0.01	0.01
Regularization (C)	0.1, 1, 10	10	0.1
RBF kernel (γ)	0.01, 0.1, 0.2	0.1	0.1
Shallow MLP			
Neurons	16, 32, 64	16	32
Epochs	10, 20, 40	20	40
Deep MLP (for all layers)			
Neurons	16, 32, 64	16	32
Epochs	10, 20, 40	10	20
Separable 2D CNN			
Filters	16, 32, 64	16	64
Kernels	(1,2), (1,3), (2,2), (3,3)	$(1,3)_{n=0}$	$(1,3)_{n=0}$
	(4,2), (5,3), (8,2), (9,3)	$(3,3)_{n>0}$	$(3,3)_{n>0}$
Epochs	10, 20, 40	20	40
LSTM			
Neurons	8, 16, 32	8	32
Epochs	10, 20, 40	20	40

Several runs of both experiments have been performed using different time window lenghts $n = [0, 4, 9, 19, 29]$, spanning the dynamics of the chillers between 1 min and 30 min.

A range of hyperparameters is established after several preliminary runs. Then, a grid search is performed to tune the hyperparameters of each model, choosing the best values in each scenario according to the results obtained with 10-fold cross validation. Table 2 summarizes the hyperparameter tuning for the best WCC2 and ACC5 models.

MLR linear approximation provides a closed-form and fast solution and does not requires tuning. The SVR method uses a radial basis function as kernel with 0.1 gamma coefficient in both models. The penalty parameter C of the error is established to 10 (WCC2 model) and 0.1 (ACC5 model) and the epsilon-tube, within which no penalty is associated in the training loss function, is set to 0.01 (in both models).

The shallow MLP method consists of 3 layers, an input layer with a dimension that depends on circuits and time, a hidden layer (16 neurons for WCC2 model and 32 neurons for ACC5 model) and an output layer (1 unit). Shallow MLP is trained with backpropagation algorithm and a rectified linear unit (ReLU) is selected as activation function. The training epochs are 20 for WCC2 model and 40 for ACC5 model. The deep MLP method consists of 12 layers, an input layer with a dimension that depends on circuits and time, 10 hidden identical layers (with 16 neurons for WCC2 model and 32 neurons for ACC5 model), and an output layer (1 unit). ReLU is again selected as activation function. The training epochs are 10 for WCC2 model and 20 for ACC5 model. As described in Section 4.2, for all the above methods the length of

the input vector is given by Variables × Circuits × Time. For that reason, the length of the input vector for the WCC2 model ranges from 5 (n=0) to 150 (n=29). On the contrary, for the ACC5 model the dimension of input data varies from 15 (n=0) to 450 (n=29).

The separable 2D CNN consists of 5 layers, an input layer (Time, Variables, Circuits), a separable 2D CNN layer comprising two convolutions, a flattening layer, a dense layer and an output layer (with a dimension of 1). For the WCC2 model, the dimension of the input data ranges from (1,5,1) (n=0) to (30,5,1) (n=29). On the contrary, for the ACC5 model the dimension of input data varies from (1,5,3) (n=0) to (30,5,3) (n=29). In the depthwise convolution, a filter kernel of (3,3) is used to detect patterns among time and variables for each circuit. Note that a kernel of (1,3) must be applied when input data contains only a timestep (n=0) and the number of depthwise convolution output channels is 16 (WCC2 model) and 64 (ACC5 model). In the pointwise convolution, a filter kernel of (1,1) is applied for all refrigeration circuits, using the same number of filters that in the depthwise convolution (16 and 64). The ReLU activation function is selected. No padding is applied, achieving feature maps with a lower dimension. No downsampling is required due to small size of input data. After the separable 2D CNN and flattening layers, a fully connected layer for processing the extracted patterns and an output layer with dimension 1 (soft sensor measurements) are used. The training epochs are set to 20 for WCC2 model and 40 for ACC5 model.

Finally, the LSTM network consists of 4 layers, an input layer (Time, Variables × Circuits), a LSTM layer with 8 neurons for WCC2 model and 32 neurons for ACC5 model, a fully connected layer with the same neurons (8 and 32) and the output layer (1 unit). For the WCC2 model, the dimension of the input data ranges from (1,5) (n=0) to (30,5) (n=29). On the contrary, for the ACC5 model the dimension of input data varies from (1,15) (n=0) to (30,15) (n=29). Both hyperbolic tangent and sigmoid are used as activation functions for all neurons. The training epochs are 20 for WCC2 model and 40 for ACC5 model.

For most methods described above, ReLU is selected as the activation function since it provided better results than Tanh and Sigmoid in all preliminary runs. Despite of some ReLU variants have provided slight improvements in previous works [54], ReLU is simple, requires low computational resources and speeds up and makes uniform the learning process [19]. A dropout regularization [44] is not used since, in general, it worsens the results, specifically for Separable 2D CNN that would require a more efficient dropout variant [9].

Experiments are executed on a PC equipped with an Intel Core i7-6700 3.40GHz CPU and 16GB RAM. No GPU memory is used.

5.4 Evaluation metrics

The MAE (Mean Absolute Error) (see Eq. 22), MAPE (Mean Absolute Percentage Error) (see Eq. 23) and R^2 (coefficient of determination) (see Eq.

24) have been selected as metrics for evaluation since their values are easily understood by any engineer [8,37].

$$MAE = \frac{1}{n}\sum_{i=1}^{n}|y_i - \hat{y}_i| \tag{22}$$

$$MAPE = \frac{100}{n}\sum_{i=1}^{n}\left|\frac{y_i - \hat{y}_i}{y_i}\right| \tag{23}$$

$$R^2 = \left(1 - \frac{\sum_{i=1}^{n}(y_i - \hat{y}_i)^2}{\sum_{i=1}^{n}(y_i - \bar{y}_i)^2}\right)100; \quad \bar{y}_i = \frac{1}{n}\sum_{i=1}^{n} y_i \tag{24}$$

Any of them provides a direct measurement of the accuracy of the soft sensor and delimits the error in the cooling production estimation.

6 Results and discussion

In this section, the results obtained for both experiments, i.e., the one with the water-cooled chiller WCC2 and the one with the air-cooled chiller ACC5, are presented.

6.1 Validating models for the soft sensor

All methods are trained and validated using a 10-fold cross validation carried out on 70% of total data for each method and both datasets (WCC2 and ACC5), considering different dynamics (including previous timesteps). Average MAE, MAPE and R^2 errors are computed, together with the standard deviations, from the 10 folds. The aim is to validate all candidate models for the soft sensor.

Table 3 presents the validation results for the WCC2 dataset, where SVR provides the lowest errors (11.37 KW with regard to 2286 kW and 1.75%) using 10 minutes of data as input. This model fits almost perfectly the cooling power data (99.80%). In the worst scenario, the MAE, MAPE and R^2 amount to 12.99 KW, 2.23% and 99.68%, which are similar to those obtained with any commercial industrial sensor. LSTM and separable 2D CNN methods also provide low percentage errors, almost always below 2%, and the cooling production estimation is fitted higher than 99%. Except for MLR, the errors do not decrease by considering longer periods of previous data. In fact, the errors are stable in the range of 1-20 minutes for SVR, Separable 2D CNN and LSTM and increase with the number of timesteps for the shallow and deep MLP.

Table 4 presents the validation results for the ACC5 dataset. In this case, the LSTM method provides the lowest errors (13.18 KW with regard to 1407 kW and 2.78%) using 5 minutes of data as input, closely followed by the separable 2D CNN (13.82 KW with regard to 1407 kW and 2.86%). According

Table 3: Validation errors for the WCC2 dataset.

WCC2 dataset	Time				
Methods	1min n=0	5min n=4	10min n=9	20min n=19	30min n=29
MAE (mean±std)					
MLR	25.62±3.59	25.27±3.57	24.83±3.50	24.01±3.44	23.27±3.39
SVR	11.95±1.50	11.42±1.64	**11.37±1.62**	11.71±1.76	11.84±1.62
Shallow MLP	13.08±2.13	13.33±3.01	14.01±3.37	15.75±3.88	15.01±1.93
Deep MLP	12.95±2.52	13.10±1.71	14.11±3.49	15.91±3.66	14.39±2.37
Sep. 2D CNN	13.02±1.97	12.73±3.42	12.90±2.09	12.90±1.72	15.69±7.53
LSTM	12.49±2.37	12.04±2.57	12.01±2.39	11.56±1.89	12.49±2.32
MAPE (mean±std)					
MLR	3.80±1.26	3.76±1.25	3.71±1.22	3.60±1.19	3.50±1.16
SVR	1.83±0.44	1.76±0.48	**1.75±0.48**	1.80±0.50	1.83±0.52
Shallow MLP	2.00±0.56	2.03±0.66	2.11±0.63	2.31±0.59	2.23±0.40
Deep MLP	1.93±0.44	2.00±0.63	2.14±0.90	2.35±0.73	2.13±0.46
Sep. 2D CNN	1.96±0.59	1.92±0.64	1.96±0.56	1.92±0.55	2.20±0.83
LSTM	1.88±0.46	1.90±0.75	1.81±0.45	1.80±0.54	1.88±0.45
R^2 (mean±std)					
MLR	98.73±0.92	98.76±0.90	98.80±0.88	98.86±0.85	98.92±0.81
SVR	99.77±0.14	99.79±0.13	**99.80±0.12**	99.78±0.13	99.77±0.14
Shallow MLP	99.71±0.18	99.71±0.17	99.68±0.17	99.54±0.33	99.64±0.15
Deep MLP	99.72±0.16	99.72±0.17	99.65±0.28	99.60±0.24	99.65±0.21
Sep. 2D CNN	99.72±0.17	99.73±0.19	99.74±0.15	99.72±0.19	99.57±0.38
LSTM	99.74±0.15	99.77±0.15	99.77±0.14	99.78±0.14	99.74±0.17

to R^2 metric, the separable 2D CNN fits the cooling power data slightly better than the LSTM (95.98% vs 94.34%). In general, the separable 2D CNN provides better results than the LSTM with other numbers of timesteps. Furthermore, separable 2D CNN brings the lowest standard deviation throughout the 10 folds. In the worst scenario, the MAE, MAPE and R^2 amount to 18.58 KW, 4.15% and 85.23% (using LSTM) or 18.55 KW, 3.91% and 92.4% (using the separable 2D CNN), which would again be considered admissible values in industrial applications. SVR also provides low absolute and percentage errors, around 15 KW and 3%, and a fairly good fit (94%). Most of the methods (except MLR and separable 2D CNN) provide higher errors as more timesteps are included as input. In general, we could argue that short periods (1-20 min) of previous data are more appropriate for the estimation of the cooling production.

Summarizing, from validation results we can observe that, on the one hand, SVR seems an appropriate method for cooling production estimation in large chillers with slow variations whereas LSTM and separable 2D CNN are noteworthy. On the other hand, both LSTM and separable 2D CNN are useful methods for estimating cooling production in small chillers with fast capacity changes and several refrigeration circuits. In general, short periods (1-20 min) of previous data provide more accurate estimations of the cooling production.

Table 4: Validation errors for the ACC5 dataset.

ACC5 dataset	Time				
Methods	1min n=0	5min n=4	10min n=9	20min n=19	30min n=29
MAE (mean±std)					
MLR	19.79±5.97	19.62±5.97	19.59±5.94	19.48±5.85	19.36±5.72
SVR	14.69±5.66	14.25±5.86	14.36±5.76	14.22±5.06	14.50±4.82
Shallow MLP	14.81±4.96	16.67±5.45	15.68±7.01	15.30±4.59	16.60±6.56
Deep MLP	14.72±4.34	15.24±5.91	15.13±5.53	15.63±5.26	17.86±5.80
Sep. 2D CNN	14.24±4.66	13.82±4.73	13.61±4.54	14.01±3.88	14.05±4.39
LSTM	14.48±6.33	**13.18±5.40**	14.42±6.59	17.04±7.23	14.60±5.47
MAPE (mean±std)					
MLR	4.19±1.57	4.18±1.59	4.18±1.58	4.16±1.58	4.14±1.56
SVR	3.11±1.47	2.98±1.47	3.00±1.41	2.98±1.22	3.07±1.15
Shallow MLP	3.07±1.22	3.48±1.31	3.30±1.71	3.26±1.27	3.46±1.63
Deep MLP	3.09±1.18	3.23±1.55	3.18±1.41	3.22±1.31	3.67±1.26
Sep. 2D CNN	2.99±1.17	2.86±1.05	2.84±1.08	2.89±0.93	2.92±1.07
LSTM	3.06±1.54	**2.78±1.37**	3.03±1.61	3.48±1.65	3.01±1.29
R^2 (mean±std)					
MLR	89.07±12.6	89.72±12.1	89.87±11.8	90.04±11.5	90.30±10.9
SVR	91.94±12.8	93.11±11.1	93.79±9.05	94.73±5.94	94.88±4.41
Shallow MLP	93.86±8.08	91.98±9.98	92.79±11.8	93.36±9.43	91.60±12.2
Deep MLP	93.55±9.44	93.33±14.3	92.81±10.9	92.69±10.1	91.01±9.69
Sep. 2D CNN	95.17±5.07	**95.98±3.58**	95.11±5.47	95.53±3.82	95.41±4.81
LSTM	93.44±10.3	94.34±9.11	92.37±13.3	92.55±8.16	94.57±6.13

6.2 Testing models for the soft sensor

After validation stage, we proceed to evaluate the models using the test set (i.e., the remaining part, 30% of the total data) of both datasets (WCC2 and ACC5). The model estimations are compared with real measurements from Fluxus F601 meter.

Table 5 presents the test results for the WCC2 dataset. Again, SVR provides the lowest MAE, MAPE and R^2 (13.22 KW, 2.36% and 99.84%, respectively), using 1 minute of data as input (although there are little differences with other selections of timesteps). It can be seen that test errors are slightly worse than validation errors for the worst case scenario, for SVR (12.99 KW, 2.23% and 99.68%) and the other methods, likely due to some novelty in the test dataset. Anyway, all the methods except MLR provide low errors comparable to any commercial industrial sensor with MAE, MAPE and R^2 around 16 KW, 3% and 99%. Again, only MLR provides lower errors as more timesteps are included as input, whereas the nonlinear methods provide slightly higher errors, with no significant differences in the range 1-10 min.

Table 6 presents the test results for the ACC5 dataset. In this case, separable 2D CNN obtains the best values of MAE, MAPE and R^2 (17.37 KW, 3.44% and 94.92%, respectively), using 30 minutes of data as input. We can observe that test errors remain in the range of the validation errors for the worst case scenario for most of the methods, especially for separable 2D CNN

Table 5: Test errors for the WCC2 dataset (30% of data).

WCC2 dataset	Time				
Methods	1min n=0	5min n=4	10min n=9	20min n=19	30min n=29
MAE					
MLR	31.96	31.21	30.38	29.00	27.91
SVR	**13.22**	13.54	13.89	14.15	14.46
Shallow MLP	14.53	15.30	15.63	17.43	17.03
Deep MLP	15.69	15.33	15.77	16.51	17.56
Sep. 2D CNN	14.85	14.72	14.73	15.91	16.80
LSTM	14.12	14.25	14.49	13.80	14.35
MAPE					
MLR	4.73	4.64	4.53	4.35	4.20
SVR	**2.36**	2.39	2.42	2.43	2.43
Shallow MLP	2.55	2.62	2.65	2.81	2.73
Deep MLP	2.72	2.73	2.71	2.81	2.95
Sep. 2D CNN	2.58	2.59	2.59	2.74	2.76
LSTM	2.48	2.56	2.49	2.43	2.50
R^2					
MLR	98.36	98.46	98.56	98.70	98.80
SVR	**99.84**	99.82	99.79	99.79	99.77
Shallow MLP	99.79	99.77	99.75	99.64	99.66
Deep MLP	99.74	99.77	99.74	99.72	99.70
Sep. 2D CNN	99.79	99.79	99.80	99.76	99.72
LSTM	99.81	99.81	99.78	99.82	99.79

(18.55 KW, 3.91% and 92.4%). In general, MLR, SVR and shallow MLP have worse results than separable 2D CNN, LSTM or even deep MLP, which are able to estimate the cooling production with a high accuracy. Moreover, separable 2D CNN provides lower errors as more timesteps are included as input, whereas MLR have higher errors as well as other nonlinear methods (SVR, shallow MLP or LSTM). Separable 2D CNN is able to extract temporal patterns efficiently, but it requires longer periods of previous data, whereas other methods achieve better results using previous data in the range of 1-10 min.

Summarizing, test results confirm the findings from validation results. On the one hand, SVR seems the best option for estimating cooling production in large chillers with slow variations although LSTM and separable 2D CNN also provide acceptable results. On the other hand, separable 2D CNN seems the best option for estimating cooling production in small chillers with fast capacity changes and several refrigeration circuits, followed by LSTM. With regard to the time window lengths, short periods (1-10 min) are in general preferable. However, there is not a clear correlation between errors and timesteps and it depends on the each method and chiller model. For example, for large chillers (WCC2), the more timesteps are considered the lower errors are obtained using MLR but the higher errors are obtained using separable 2D CNN. On the contrary, for small chillers (ACC5), the more timesteps are considered the higher errors are obtained using MLR but the lower errors are obtained using separable 2D CNN. Indeed, in this case (ACC5 dataset) the separable

Table 6: Test errors for the ACC5 dataset (30% of data).

ACC5 dataset	Time				
Methods	1min n=0	5min n=4	10min n=9	20min n=19	30min n=29
MAE					
MLR	28.04	28.92	29.23	30.97	31.60
SVR	19.05	18.89	19.58	19.86	21.13
Shallow MLP	19.10	18.45	18.39	19.09	22.89
Deep MLP	18.65	19.49	18.24	18.82	18.61
Sep. 2D CNN	17.57	17.95	17.92	19.06	**17.37**
LSTM	17.99	17.93	17.44	18.55	19.20
MAPE					
MLR	6.26	6.51	6.59	7.11	7.30
SVR	4.36	3.93	3.96	4.00	4.24
Shallow MLP	3.97	3.86	3.89	4.15	4.89
Deep MLP	3.72	3.87	3.63	3.78	3.75
Sep. 2D CNN	3.63	3.58	3.54	3.74	**3.44**
LSTM	3.72	3.70	3.59	3.80	3.89
R^2					
MLR	85.31	83.49	82.86	71.49	66.24
SVR	92.83	94.46	94.42	93.99	92.85
Shallow MLP	93.66	94.30	94.04	91.18	86.67
Deep MLP	94.28	93.43	94.73	94.46	94.34
Sep. 2D CNN	94.84	94.91	94.85	94.02	**94.92**
LSTM	94.60	94.88	94.90	94.43	93.84

2D CNN provides better results with 30 min. It takes better coherence of the spatio-temporal relationships in complex data structures (modular chillers with several circuits and longer time windows).

The aim of this study is to select the most appropriate model in order to build a soft sensor which estimates cooling production in chillers. A versatile soft sensor should provide good estimations regardless the kind of chiller. For that reason, **separable 2D CNN** will be chosen, since it was found the best option for small chillers with several refrigeration circuits and the third option for larger chillers.

Fig. 5 shows the test results (30% data) of cooling production estimation for both chillers (WCC2 and ACC5) using separable 2D CNN (with a time window of 1 and 30 min, respectively). For WCC2 (see Fig. 5a), cooling power can be estimated with MAE, MAPE and R^2 of 14.85 KW (with regard to 2286 kW), 2.57% and 99.79%. This accuracy encourages to deploy the soft sensor, instead of installing a real sensor in the output pipe. For ACC5 (see Fig. 5b), MAE, MAPE and R^2 are 17.37 KW (with regard to 1407 kW), 3.44% and 94.92%. In this case, the accuracy worsens slightly due to the number of changes in chiller capacity, needed to cover a varying building cooling load. However, it can still be considered admissible. Furthermore, errors are clearly lower when focusing only on stable regions.

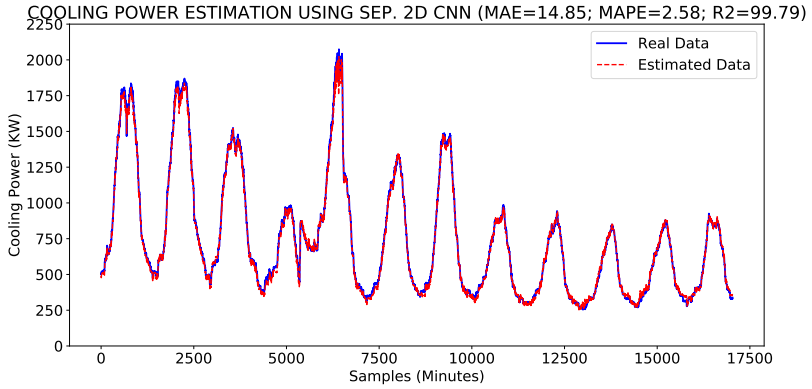

a Water-cooled chiller (WCC2).

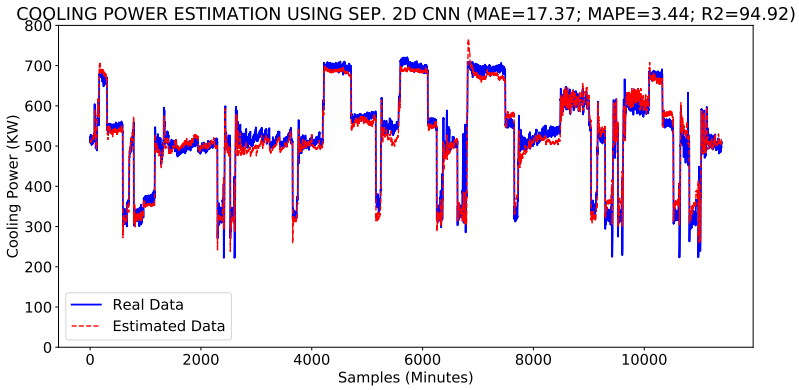

b Air-cooled chiller (ACC5).

Fig. 5: Cooling production estimation using the soft sensor (separable 2D CNN).

6.3 Monitoring COP using the soft sensor

The final aim of the soft sensor is to assess the chiller efficiency. For that purpose, the estimated COP value is reported, computed using the cooling power estimation and the measured electric power for the test set of both chillers (WCC2 and ACC5). Fig. 6 shows the COP ranges for both chillers.

For WCC2 (see Fig. 6a), estimated COP spans from 2.6 to 8, being its average 5.25. Extreme values correspond to unstable periods such as chiller starts/stops and to low cooling capacities, what certainly worsens the efficiency in large chillers. Although the refrigerant conditions are slightly different, the average COP (5.25) is lower than the nominal value (6.23). Moreover, that chiller runs for a long time with a COP below the average value. This situation reveals an amendable operation, especially with low cooling capaci-

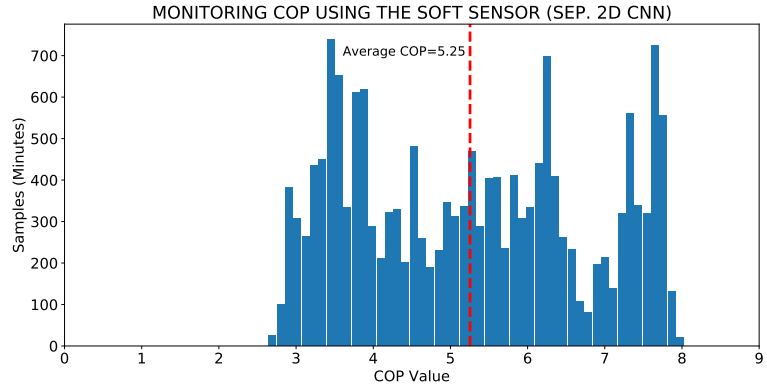

a Water-cooled chiller (WCC2).

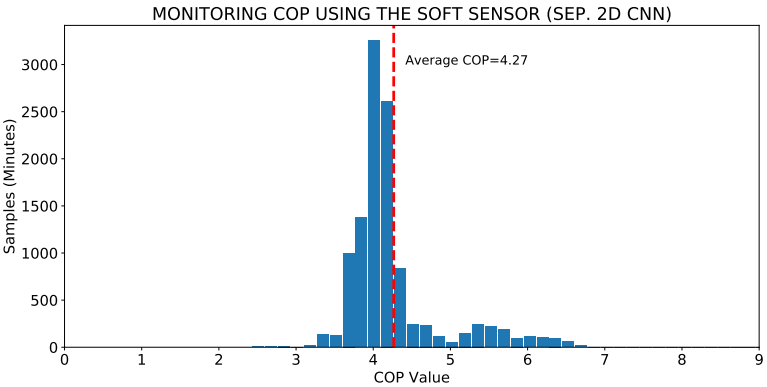

b Air-cooled chiller (ACC5).

Fig. 6: Monitoring COP using the soft sensor.

ties. Therefore, actions lead to improve the operation of this chiller should be carried out.

For ACC5 (see Fig. 6b), estimated COP spans from 2.6 to 6.8, being its average 4.27. In this case, COP values are more concentrated around the average value, revealing a more efficient operation. Furthermore, the average COP (4.27) is almost equal to the nominal value (4.3), despite slightly different refrigerant conditions. Note that extreme values correspond mainly to chiller starts/stops.

7 Conclusions

In this paper, a methodology is proposed to build a soft sensor, which allows us to estimate cooling production and monitoring efficiency in chillers. It requires a relatively low-cost and simple infrastructure. During the production period,

the estimation of the cooling production is done in the inference phase of the designed model, thereby demanding low computational effort. For training and testing periods, however, it involves more computational resources, as well as the exceptional availability of a portable cooling power meter to measure and record actual cooling power data under a range of conditions. The proposed soft sensor uses independent variables, such as internal states of the chillers (temperatures and pressures of the refrigeration gas) and input electric power, for the estimation of cooling power. The development of the soft sensor can benefit from current or past observations of those independent variables.

Six methods (MLR, SVR, shallow MLP, deep MLP, separable 2D CNN and LSTM) are considered to develop the model for the soft sensor. A 10-fold validation is performed to set their hyperparameters and, after test stage, the most appropriate method (according to MAE, MAPE and R^2 metrics) is chosen to implement the soft sensor. Experiments have been performed using two different chillers located at the Hospital of León (one water-cooled and one air-cooled chiller).

Deep learning methods, such as separable 2D CNN and LSTM, seem promising with relative errors from 2.5% to 3.5% in the cooling production estimation and justify the use of the soft sensor in real installations. Although, for large chillers with slow dynamics and one refrigeration circuit, traditional methods such as SVR can provide accurate measurements, even with a lower computational cost than deep learning methods, they are not as successful for the estimation of cooling production in small chillers with fast dynamics and many refrigeration circuits. On the contrary, deep learning methods such as separable 2D CNN provide accurate measurements for both small and large chillers, considering different timesteps in each case. Separable 2D CNN takes advantage of the structure of data (time, variables and refrigeration circuits), providing excellent results in all scenarios and so it is the method chosen to build the soft sensor.

The development of the soft sensor is valuable for several reasons: First, the estimations of the soft sensor can avoid the installation of expensive industrial flow and energy meters or can replace portable measuring systems. Second, the estimation of cooling power (output) together with the electric power (input) enables monitoring and tracking the efficiency in chillers. In this paper, COP is chosen as the energy efficiency indicator and so the histogram with COP values is presented for both chillers. Third, this methodology can be applicable to any chiller, resulting in a low cost and easy approach to monitor its efficiency.

As future work, it would be interesting to analyze a finer-grain selection of hyperparameters, which might lead to more accurate conclusions about their effect in the performance. Furthermore, this work can be extended by implementing the best-performing model in a low-cost embedded board in order to develop a prototype of portable sensor, which can be deployed in production environments. The implementation of the soft sensor would require deploying and running the models into a single-board computer, adjusting sensor parameters and communicating with the chiller control board or building management system to acquire independent variables.

Conflict of interest

The authors declare that they have no conflict of interest.

References

1. Abdel-Nasser, M., Mahmoud, K.: Accurate photovoltaic power forecasting models using deep LSTM–RNN. Neural Computing and Applications **31**(7), 2727–2740 (2019). DOI 10.1007/s00521-017-3225-z
2. Ahmed, T.: Chapter 7 – Equations of state. In: T. Ahmed (ed.) Working Guide to Vapor–liquid Phase Equilibria Calculations, pp. 59 – 96. Gulf Professional Publishing, Boston (2010). DOI 10.1016/B978-1-85617-826-6.00007-8
3. Alonso, S., Morán, A., Pérez, D., Reguera, P., Díaz, I., Domínguez, M.: Virtual sensor based on a deep learning approach for estimating efficiency in chillers. In: J. Macintyre, L. Iliadis, I. Maglogiannis, C. Jayne (eds.) Engineering Applications of Neural Networks, pp. 307–319. Springer International Publishing, Cham (2019)
4. Alves, O., Monteiro, E., Brito, P., Romano, P.: Measurement and classification of energy efficiency in HVAC systems. Energy and Buildings **130**, 408 – 419 (2016). DOI 10.1016/j.enbuild.2016.08.070
5. Bechtler, H., Browne, M., Bansal, P., Kecman, V.: New approach to dynamic modelling of vapour-compression liquid chillers: artificial neural networks. Applied Thermal Engineering **21**(9), 941 – 953 (2001). DOI 10.1016/S1359-4311(00)00093-4
6. Beghi, A., Brignoli, R., Cecchinato, L., Menegazzo, G., Rampazzo, M., Simmini, F.: Data-driven fault detection and diagnosis for hvac water chillers. Control Engineering Practice **53**, 79–91 (2016)
7. Bishop, C.M., et al.: Neural networks for pattern recognition. Oxford university press (1995)
8. Bowerman, B., O'Connell, R., Koehler, A.: Forecasting, Time Series, and Regression: An Applied Approach. Duxbury advanced series in statistics and decision sciences. Thomson Brooks/Cole (2005)
9. Cai, S., Gao, J., Zhang, M., Wang, W., Chen, G., Ooi, B.C.: Effective and efficient dropout for deep convolutional neural networks. CoRR **abs/1904.03392** (2019). URL http://arxiv.org/abs/1904.03392
10. Chang, Y.C.: Sequencing of chillers by estimating chiller power consumption using artificial neural networks. Building and Environment **42**(1), 180 – 188 (2007). DOI 10.1016/j.buildenv.2005.08.033
11. Chollet, F.: Xception: Deep learning with depthwise separable convolutions. In: 2017 IEEE Conference on Computer Vision and Pattern Recognition (CVPR), pp. 1800–1807 (2017). DOI 10.1109/CVPR.2017.195
12. Ciresan, D., Meier, U., Gambardella, L., Schmidhuber, J.: Deep big multilayer perceptrons for digit recognition. In: G. Montavon, G. Orr, K. Müller (eds.) Neural Networks: Tricks of the Trade, vol. 7700, pp. 581–598. Springer, Berlin, Heidelberg (2012)
13. Comstock, M.C., Braun, J.E., Bernhard, R.: Experimental data from fault detection and diagnostic studies on a centrifugal chiller. Purdue University (1999)
14. Cortes, C., Vapnik, V.: Support-vector networks. Machine Learning **20**(3), 273–297 (1995)
15. Fan, C., Sun, Y., Zhao, Y., Song, M., Wang, J.: Deep learning-based feature engineering methods for improved building energy prediction. Applied Energy **240**, 35 – 45 (2019). DOI 10.1016/j.apenergy.2019.02.052
16. Fan, C., Xiao, F., Zhao, Y.: A short-term building cooling load prediction method using deep learning algorithms. Applied energy **195**, 222–233 (2017)
17. Fu, G.: Deep belief network based ensemble approach for cooling load forecasting of air-conditioning system. Energy **148**, 269 – 282 (2018). DOI 10.1016/j.energy.2018.01.180
18. Ge, Y., Wu, H.: Prediction of corn price fluctuation based on multiple linear regression analysis model under big data. Neural Computing and Applications (2019). DOI 10.1007/s00521-018-03970-4

19. Glorot, X., Bordes, A., Bengio, Y.: Deep sparse rectifier neural networks. In: Proceedings of the fourteenth international conference on artificial intelligence and statistics, pp. 315–323 (2011)
20. Goodfellow, I., Bengio, Y., Courville, A.: Deep Learning. MIT Press (2016). http://www.deeplearningbook.org
21. Gordon, J.M., Ng, K.C.: Cool Thermodynamics: The Engineering and Physics of Predictive, Diagnostic and Optimization Methods for Cooling Systems. Cambridge International Science Publishing (2000)
22. Hastie, T., Tibshirani, R., Friedman, J.: The elements of statistical learning. Second Edition. Springer (2009)
23. Haykin, S.S.: Neural networks and learning machines. 3rd Edition. Pearson Education (2009)
24. Hochreiter, S., Schmidhuber, J.: Long short-term memory. Neural Computation **9**(8), 1735–1780 (1997). DOI 10.1162/neco.1997.9.8.1735
25. Huang, G., Sun, Y., Wang, S.: Building instantaneous cooling load fused measurement: Multiple-sensor- based fusion versus chiller-model-based fusion. Building Services Engineering Research and Technology **34**, 177–194 (2013). DOI 10.1177/0143624411432651
26. Huang, G., Wang, S., Sun, Y.: Enhancing the reliability of chiller control using fused measurement of building cooling load. HVAC&R Research **14**(6), 941–958 (2008)
27. Jolliffe, I.: Principal component analysis. Springer (2011)
28. Kadlec, P., Gabrys, B., Strandt, S.: Data-driven soft sensors in the process industry. Computers & Chemical Engineering **33**(4), 795 – 814 (2009). DOI 10.1016/j.compchemeng.2008.12.012
29. Klein, S.A.: Design considerations for refrigeration cycles. In: International Refrigeration and Air Conditioning Conference, vol. 190, pp. 511 – 519. Purdue e-Pubs (1992). URL http://docs.lib.purdue.edu/iracc/190
30. Li, H., Yu, D., Braun, J.E.: A review of virtual sensing technology and application in building systems. HVAC&R Research **17**(5), 619–645 (2011). DOI 10.1080/10789669.2011.573051
31. Liu, L., Kuo, S.M., Zhou, M.: Virtual sensing techniques and their applications. In: 2009 International Conference on Networking, Sensing and Control, pp. 31–36. IEEE (2009)
32. Ma, W., Fang, S., Su, B., Xue, X., Li, M.: Second-law-based analysis of vapor-compression refrigeration cycles: Analytical equations for cop and new insights into features of refrigerants. Energy Conversion and Management **138**, 426 – 434 (2017). DOI 10.1016/j.enconman.2017.02.017
33. Mandard, E., Kouame, D., Battault, R., Remenieras, J., Patat, F.: Methodology for developing a high-precision ultrasound flow meter and fluid velocity profile reconstruction. IEEE Transactions on Ultrasonics, Ferroelectrics, and Frequency Control **55**(1), 161–172 (2008). DOI 10.1109/TUFFC.2008.625
34. Mcdonald, E., Zmeureanu, R.: Virtual flow meter to estimate the water flow rates in chillers. ASHRAE Transactions **120**, 200–208 (2014)
35. McDonald, E., Zmeureanu, R.: Development and testing of a virtual flow meter tool to monitor the performance of cooling plants. Energy Procedia **78**, 1129 – 1134 (2015). DOI 10.1016/j.egypro.2015.11.071
36. McIntosh, I.B., Mitchell, J.W., Beckman, W.A.: Fault detection and diagnosis in chillers–part i: Model development and application/discussion. ASHRAE Transactions **106**, 268 (2000)
37. Menard, S.: Coefficients of determination for multiple logistic regression analysis. The American Statistician **54**(1), 17–24 (2000). DOI 10.1080/00031305.2000.10474502
38. Moran, M.J., Shapiro, H.N., Boettner, D.D., Bailey, M.B.: Principles of Engineering Thermodynamics. John Wiley & Sons Inc (2015)
39. Muhammad Ehsan, R., Simon, S.P., Venkateswaran, P.R.: Day-ahead forecasting of solar photovoltaic output power using multilayer perceptron. Neural Computing and Applications **28**(12), 3981–3992 (2017). DOI 10.1007/s00521-016-2310-z
40. Pérez-Lombard, L., Ortiz, J., Pout, C.: A review on buildings energy consumption information. Energy and Buildings **40**(3), 394 – 398 (2008). DOI 10.1016/j.enbuild.2007.03.007

41. Reddy, T.A., Niebur, D., Andersen, K.K., Pericolo, P.P., Cabrera, G.: Evaluation of the suitability of different chiller performance models for on-line training applied to automated fault detection and diagnosis (rp-1139). HVAC&R Research **9**(4), 385–414 (2003). DOI 10.1080/10789669.2003.10391077
42. Saha, P., Debnath, P., Thomas, P.: Prediction of fresh and hardened properties of self-compacting concrete using support vector regression approach. Neural Computing and Applications (2019). DOI 10.1007/s00521-019-04267-w
43. Saidur, R., Hasanuzzaman, M., Mahlia, T., Rahim, N., Mohammed, H.: Chillers energy consumption, energy savings and emission analysis in an institutional buildings. Energy **36**(8), 5233 – 5238 (2011). DOI 10.1016/j.energy.2011.06.027. PRES 2010
44. Srivastava, N., Hinton, G., Krizhevsky, A., Sutskever, I., Salakhutdinov, R.: Dropout: a simple way to prevent neural networks from overfitting. The Journal of Machine Learning Research **15**(1) (2014). DOI 10.5555/2627435.2670313
45. Stratistics Market Research Consulting: Modular chillers – Global market outlook (2018-2027). Tech. Rep. 4844759, Research and Markets (2019)
46. Swider, D., Browne, M., Bansal, P., Kecman, V.: Modelling of vapour-compression liquid chillers with neural networks. Applied Thermal Engineering **21**(3), 311 – 329 (2001). DOI 10.1016/S1359-4311(00)00036-3
47. Teke, A., Timur, O.: Assessing the energy efficiency improvement potentials of HVAC systems considering economic and environmental aspects at the hospitals. Renewable and Sustainable Energy Reviews **33**(Supplement C), 224 – 235 (2014). DOI 10.1016/j.rser.2014.02.002
48. Tian, C., Xing, Z., Pan, X., Tian, Y.: A method for cop prediction of an on-site screw chiller applied in cinema. International Journal of Refrigeration **98**, 459–467 (2019). DOI 10.1016/j.ijrefrig.2018.10.020
49. Wang, B., Lei, Y., Li, N., Yan, T.: Deep separable convolutional network for remaining useful life prediction of machinery. Mechanical Systems and Signal Processing **134**, 106330 (2019)
50. Wang, H.: Water flow rate models based on the pipe resistance and pressure difference in multiple parallel chiller systems. Energy and Buildings **75**, 181 – 188 (2014). DOI 10.1016/j.enbuild.2014.02.017
51. Wang, H.: Empirical model for evaluating power consumption of centrifugal chillers. Energy and Buildings **140**, 359 – 370 (2017). DOI 10.1016/j.enbuild.2017.02.019
52. Wang, S., Cui, J.: Sensor-fault detection, diagnosis and estimation for centrifugal chiller systems using principal-component analysis method. Applied Energy **82**(3), 197–213 (2005)
53. Wang, S., Cui, J.: A robust fault detection and diagnosis strategy for centrifugal chillers. HVAC&R Research **12**(3), 407–428 (2006)
54. Xu, B., Wang, N., Chen, T., Li, M.: Empirical evaluation of rectified activations in convolutional network. arXiv preprint arXiv:1505.00853 (2015)
55. Yu, F., Chan, K.: Part load performance of air-cooled centrifugal chillers with variable speed condenser fan control. Building and Environment **42**(11), 3816 – 3829 (2007). DOI 10.1016/j.buildenv.2006.11.029
56. Yu, F., Chan, K.: Improved energy management of chiller systems with data envelopment analysis. Applied Thermal Engineering **50**(1), 309 – 317 (2013). DOI 10.1016/j.applthermaleng.2012.08.023
57. Yu, F., Chan, K., Sit, R., Yang, J.: Review of standards for energy performance of chiller systems serving commercial buildings. Energy Procedia **61**, 2778 – 2782 (2014). DOI 10.1016/j.egypro.2014.12.308
58. Zhao, X., Yang, M., Li, H.: Development, evaluation and validation of a robust virtual sensing method for determining water flow rate in chillers. HVAC&R Research **18**(5), 874–889 (2012). DOI 10.1080/10789669.2012.667036